Two-phase Modelling of Bridge Pier Scour during Flood Event

Bing Chen[1]

[1] School of Civil Engineering, Shandong Jiaotong University, Haitang Road 5001, Shandong province, China; e-mail: chenbing142857@tju.edu.cn

ABSTRACT

Pier scour has been recognized as one of the main threats to bridge safety. Most studies about bridge pier scour were carried out using single-phase numerical models, which calculate the total sediment transport with assumption of bedload and suspended sediment transport separately, among them were the bedload sediment transport formulae adopted in those models mainly derived from steady flow experiments. For a better understanding of the mechanics of local scour under unsteady flow conditions such as flood events, a three-dimensional Euler-Euler two-phase model was implemented for simulating flood-induced scour around a circular pier on sand bed. This simulation was focused on the scour progress, the shape of scour hole, and the maximum scour depth during the whole flood event. Model results provided more details of scour progress, and were used to explain the mechanics of scour in varying flow conditions during the flood event.

Keywords: bridge pier scour, flood event, numerical simulation, Eulerian-Eulerian two-phase model

INTRODUCTION

Local scour is one of the main causes of the collapse of bridge piers. More than 60% bridge collapse due to local scour in America (Briaud et al. 1999). It is a function of bed material size, flow characteristics, fluid properties and the geometry of the bridge pile. Theoretical and experimental studies were carried out for many years. Dozens of empirical formulae were established for equilibrium scour depth, based on plenty of experimental results and few field survey data (Richardson et al. 1993; Sumer and Fredsøe 2002). Those formulae were mainly for predicting the equilibrium scour depth, which was obtained in experiments by the assumption that the duration of flow velocity lasting long enough. However, the time evolution of scour and filling phenomena has not received much attention, especially in unsteady flow conditions. In the flood season, flood duration may be not as long as the time needed to achieve equilibrium scour. The flow discharge was large and fast time-varying. In such cases, scour can quickly reach great depths, thereby threatening the stability of a bridge pier and causing its collapse (Federico et al. 2003).

Field scour depths were often measured after the flood had occurred and the depths were not representative of the flow conditions that caused them. In the recent years, some studies (Su

and Lu 2013; Hong et al. 2015) measured bridge pier scour during the flood event in rivers. Link et al. (2016) carried out four series of experimental tests to study the effects of different hydrograph with short and long durations on time-dependent scour depth and scour rate. Most studies about local scour modelling were carried out by means of single-phase numerical models (Roulund et al. 2005, Liu and García 2008), which calculate the total sediment transport with assumption of bedload and suspended sediment separately. Suspended sediment transport was calculated via the sediment transport equation, and the bedload transport was calculated via empirical bedload sediment transport formulae (e.g., Engulund and Fredsøe 1976, Van Rijn 1984), which are derived by experiments in steady flow situations.

The advantage of two-phase model that the approach does not require to use the empirical sediment transport rate and erosion- deposition laws and no additional equation has to be solved for the bed evolution (Exner equation). Recently, an open-source multi-dimensional Reynolds-averaged two-phase sediment transport model, sedFoam has been proposed by Cheng et al. (2014). So far, this Eulerian-Eulerian two-phase model sedFoam has been validated in sheet flow condition, momentary bed failure (Cheng et al. 2017), and scour downstream of an apron (Chauchat et al. 2017). Mathieu et al. (2019) used sedFoam to simulate the lee-wake erosion of scour below a submarine pipeline. Nagel et al. (2017) used sedFoam to simulate the local scour around a cylindrical pile, and the experimental results of Roulund et al. (2005) was adopted for validation in steady flow condition.

Despite its importance of bridge design work, however, scour caused by flood waves have not been investigated extensively. The present study attempted to simulate scour processes of the time-dependent scour during flood waves. One experimental result of Link et al. (2016) was used for validation. This study aims to study the time-dependent scour properties such as scour depth development, shape of scour hole and scour rate under unsteady hydraulic conditions.

NUMERICAL MODEL AND SET-UP

In the present study the two-phase flow computations were performed using sedFoam, which was established based on open source codes OpenFOAM. Multiple numerous solvers, discretization schemes and utilities were provided in OpenFOAM. The model sedFoam has been validated in cylinder flow and scour under steady current (Nagel et al. 2017). In the present study, the model was used to validate the situations of the non-uniform conditions, such as a flood event.

The mass conservation equations for the particle phase and fluid phase in the Eulerian two-phase model sedFoam (Cheng et al. 2017, Chauchat et al. 2017) are written as the following:

$$\frac{\partial \alpha}{\partial t} + \frac{\partial \alpha u_i^a}{\partial x_i} = 0 \tag{1}$$

$$\frac{\partial \beta}{\partial t} + \frac{\partial \beta u_i^b}{\partial x_i} = 0 \tag{2}$$

Where α and β are the sediment particle and fluid concentration, u_i^a, u_i^b are the sediment and fluid velocities, respectively.

The momentum equations for fluid and particle phases can be written as the following:

$$\frac{\partial \rho^a \alpha u_i^a}{\partial t} + \frac{\partial \rho^a \alpha u_i^a u_j^a}{\partial x_j} = -\alpha \frac{\partial p}{\partial x_i} + \alpha f_i - \frac{\partial \tilde{p}^a}{\partial x_i} + \frac{\partial \tau_{ij}^a}{\partial x_j} + \alpha \rho^a g_i + \alpha\beta K(u_i^b - u_i^a) - S_{us}\beta K \nu_t^b \frac{\partial \alpha}{\partial x_i} \quad (3)$$

$$\frac{\partial \rho^b \beta u_i^b}{\partial t} + \frac{\partial \rho^b \beta u_i^b u_j^b}{\partial x_j} = -\beta \frac{\partial p}{\partial x_i} + \beta f_i + \frac{\partial \tau_{ij}^b}{\partial x_j} + \beta \rho^b g_i - \alpha\beta K(u_i^b - u_i^a) + S_{us}\beta K \nu_t^b \frac{\partial \alpha}{\partial x_i} \quad (4)$$

Where the superscript *a* and *b* represent sediment and fluid phase variables, respectively. *p* is the fluid pressure, τ_{ij}^b is fluid stress including fluid grain-scale (viscous) stress and fluid Reynolds stresses. $\tilde{p}^a$ ($\tilde{p}^a = p^{ff} + p^a$) is the sediment particle pressure, p^{ff} is permanent contact component of the particle pressure, and p^a is collisional component of particle pressure. τ_{ij}^a is the sediment shear stress. The last two terms on the right-hand side of equation 3 and 4 are momentum coupling between the sediment and fluid phase through drag force, where *K* is the drag parameter. The typical flow patterns around a circular cylinder structure foundation in the river are the contraction of the flow at the lateral side, the downstream flow in the front of cylinder, the horseshoe vortices in the front and lateral side, and the lee vortices in the downstream side. A k −ω turbulence model was chosen in the present simulation. More comprehensively descriptions of the coefficients computation and discrete methods in model sedFoam can be seen in Chauchat et al. (2017).

Link et al. (2016) carried out four series of experimental tests in an in-floor rectangular flume of 26m long, 1.5m wide, and 0.74m deep at the Laboratory with a pile diameter D = 0.15m mounted in the middle of a sediment-recess. Dimensionless particle diameter D* is 9, the relative density is 1.65, and the standard deviation of the sediment grain size is 1.45. Median size of sediment d_{50}=0.36mm. The case A-2 was adopted in the present study for validation.

In order to reduce the runtime, the computational domain was set to 15D (D is pile diameter, set to 0.05m in the present simulation) in the *x* direction, 10D in *y* direction, water depth was equal to 0.21m, which was the same as Link et al. (2016) experiment. The sediment layer height was equal to 0.1m in the *z* direction. A hyperbolic tangent profile of sediment concentration was used for initial conditions.

The snappyHexMesh tool was used to generate the grid, which was refined in the cylinder region. The horizontal resolution of the present grid was about 3.75×10^{-3} m, totally 60 layers in the vertical direction, and the total number of the grid for in computation area were 1333970. At the walls (e.g., pile; bottom bed), a boundary layer mesh type was used. The boundary conditions are shown in Figure 1. The *k*-ω model was adopted for turbulent simulation. At the walls, ω was imposed via wall functions. More details of the *k*-ω model in sedFoam can be found in Chauchat et al. (2017). Gauss limited linear scheme was used for advection terms, Gauss linear corrected scheme was used for Laplacian terms, Gauss linear scheme was used for gradient terms, and the Euler implicit scheme was used for time discretization.

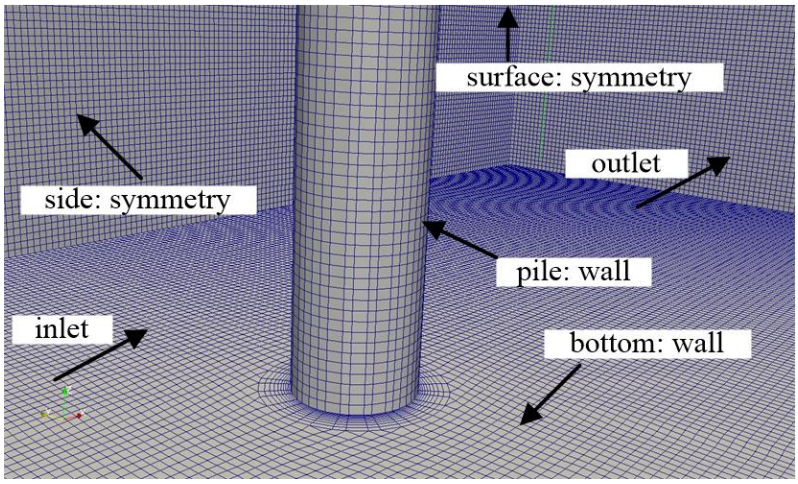

Figure 1. Sketch of the boundary conditions in present numerical model.

The inlet boundary condition was implemented by time-varying flow discharge, and the hydrograph of series A-2 in Link et al. (2016) was adopted. The width of computation domain was 0.5m, the flow discharge was reduced based on the flood hydrograph used by Link et al. experiment (Figure 2). The initial condition at the inlet was imposed via a 1D profiles computed with boundaryFoam. For outlet, a standard boundary condition named OutletInletVelocity boundary condition was used, which switches between the zero gradient and the fixed value. The top surface and sidewalls were set to symmetry boundary conditions. The pile surface and bottom bed were set to walls (Figure 1), and wall function was employed in the turbulent computation.

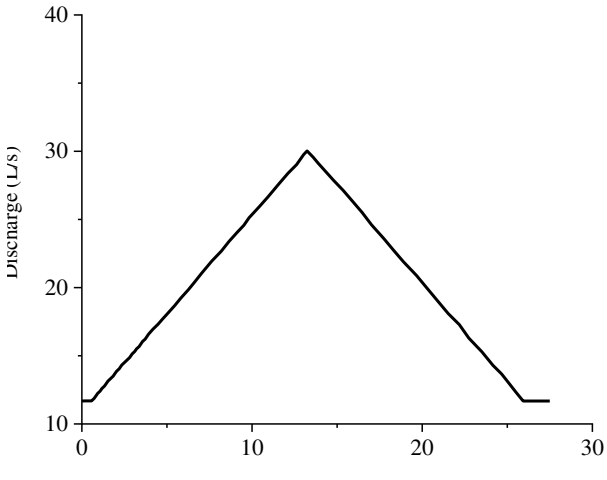

Figure 2. Hydrograph implemented at the inlet boundary in the present study.

RESULTS AND DISSCUSSION

The typical flow field around a circular cylinder was reproduced in the present study. Instantaneous flow streamlines were showed in Figure 3. The horseshoe vortex, contraction of flow in the lateral side and the lee-wake vortices were captured well. As the velocity increased with the increasing flow discharge implemented in the inlet boundary, the flow field changed consequently.

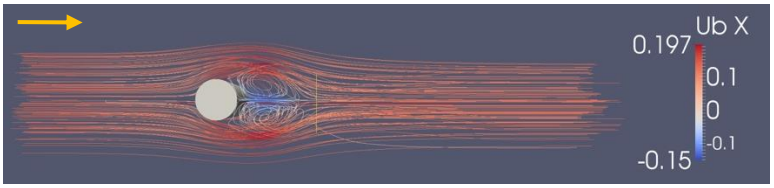

Figure 3. Snapshot of instantaneous fluid phase velocity streamline.

Scour depth was obtained by the value of sediment particle concentration α. Figure 4 depicted the side view of the distribution of alpha in the computation area. For the sediment diameter used here, the critical velocity critical velocity for incipient motion of sediment particles was about 0.32m/s. In the present study, flow velocities obtained from flow discharge ranged from 0.12~0.31m/s, which is a little smaller than the critical velocity of sediment grain ensuring the scour type being in clear-water scour regime.

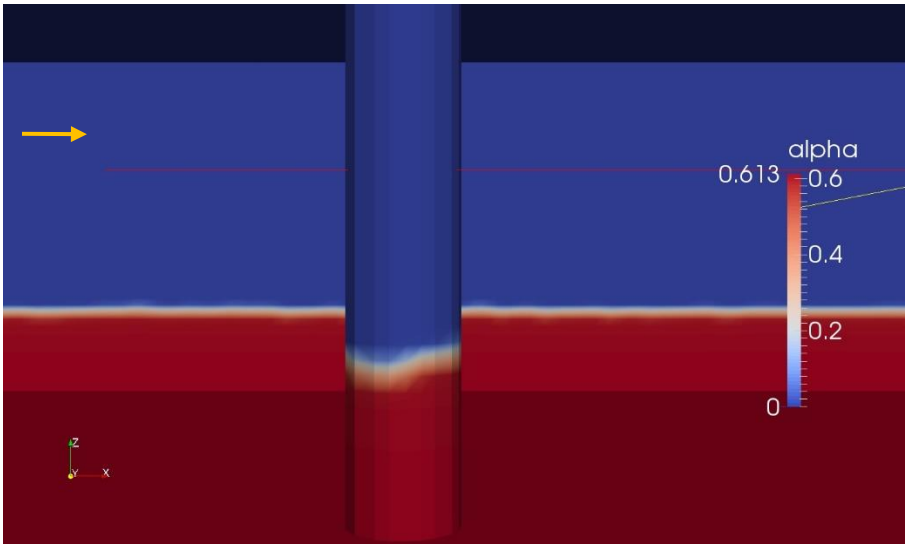

Figure 4. Snapshot of values of alpha around the pile.

The time-varying shapes of scour hole were showed in Figure 5. At the early time, scour occurred at the lateral side of pile due to the contraction of flow. The increased shear stress near the pile leads to erosion. The scour hole area expanded with increasing flow velocity and flow duration time. It should be noticed that the only erosion depth was included for clearness in Figure 5.

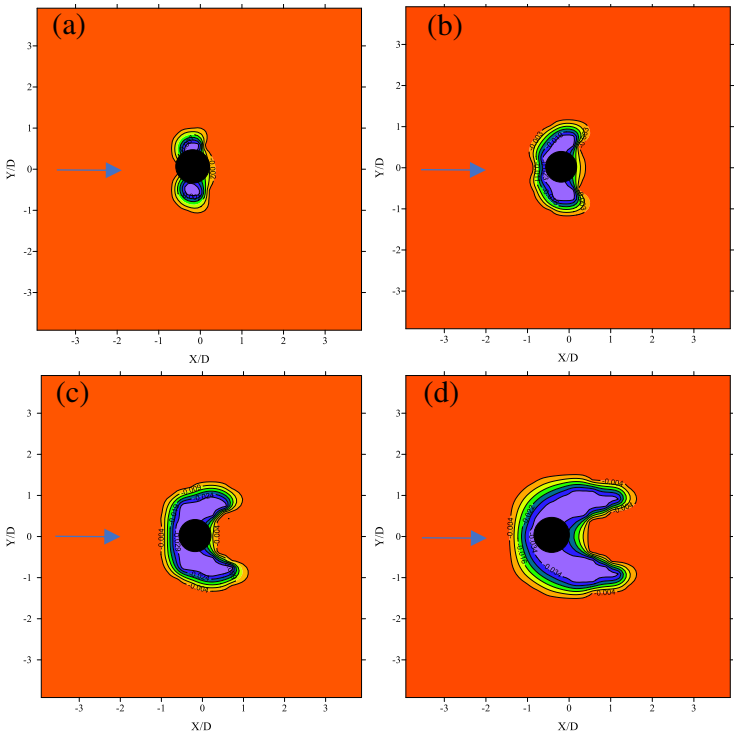

Figure 5. Contour of scour depth in different time.

The time-dependent scour depth was showed in Figure 6. In the early time, flow velocity was small, the ratio of average flow velocity to critical velocity for incipient motion of sediment particles was even smaller than 0.5. The flow condition was not strong enough, and the scour did not happen. When the flow velocity increased with the increasing flow discharge, the scour progresses started. In the later time, the scour depth remained the same because the flow velocity decreased with the descending flow discharge, the flow intense was not strong enough to move the sediment particles inside the scour hole since larger shear stress was needed for sediment on the slope.

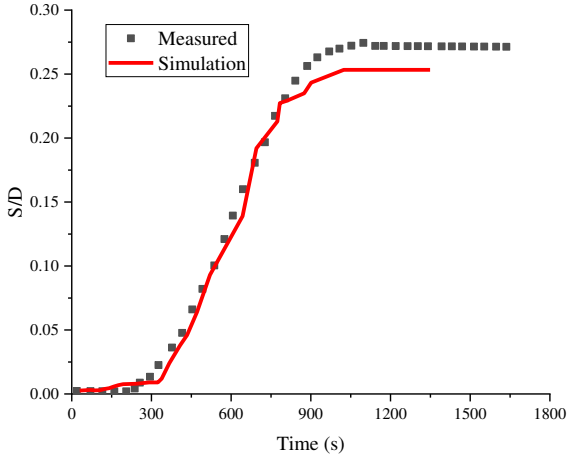

Figure 6. Time-varying scour depth in the nose of the cylinder.

The finally scour hole can be seen in Figure 7. The largest scour depth occurred at the front of the pile, and the deposition of sediments occurred in the lee side. The shape of scour hole was similar to situations under steady flow, while, the scour depth ($\approx 0.27D$) was much smaller than equilibrium scour depth ($\approx 1.5D$) based on equilibrium scour depth formulae. It is expected that scour depth under flood event not only be relevant to flow discharge, but also the duration of the peak flow velocity.

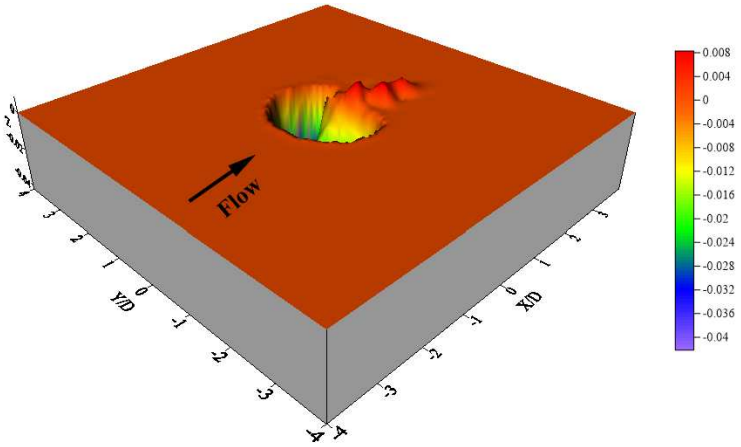

Figure 7. 3D surface map of scour hole.

It should be pointed that only clear-water local scour was taken account in the present simulation. For live-bed scour situation, the time-varying scour depth will show different pattern because of the effects of sand dunes movement. Bridge vulnerability during flood event is a complicated problem. More simulation about complicated shape foundations and flow conditions should be proposed in the future work. Details of the flow field and the sediment movements should be discussed.

CONCLUSION

In the present study, a 3D Eulerian-Eulerian two-phase model sedFoam was used to simulate clear-water local scour around a circular cylinder under a flood event. It is a primitive attempting to use two-phase model to simulate scour under flood events conditions. Comparisons between the simulation results and the experimental observations showed that the two-phase model can be used in the unsteady conditions. The scour depth of some degree in line with experimental results, there is still some discrepancy in the shape of scour hole. Different grid resolutions used in simulation affected the model stability and the scour hole shape significantly. Scour depth under flood event was not only being relevant to flow discharge, but also the duration of peak flow velocity.

ACKNOWLEDGEMENT

This work was supported by the Scientific and Technological Research Program of Chongqing Municipal Education Commission (No: KJQN201803808).

REFERENCES

Briaud, J. L., Ting F. C., Chen H., Gudavallir R., Peregu S., Wei G. (1999). "Sricos: Prediction of scour rate in cohesive soils at bridge piers". *J. Geotech. Geoenviron. Eng.*, 125(4), 237-246.

Chauchat, J., Cheng, Z., Nagel, T., Bonamy, C., and Hsu, T. J. (2017). "SedFoam-2.0: a 3-D two-phase flow numerical model for sediment transport." *Geosci. Model Dev.*, 10(12), 4367-4392.

Cheng, Z., and Hsu, T. J. (2014). *A multi-dimensional two-phase eulerian model for sediment transport-twophaseeulersedfoam (version 1.0)*. In Tech. Rep CACR-14-08. University of Delaware.

Cheng, Z., Hsu, T.-J., and Calantoni, J. (2017). "SedFoam: A multidimensional Eulerian two-phase model for sediment transport and its application to momentary bed failure." *Coast. Eng*., 119, 32-50.

Engelund, F., Fredsøe, J. (1976). "A sediment transport model for straight alluvial channels." *Hydrol. Res*., 7(5), 293-306.

Federico, F., Silvagni, G., Volpi F. (2003). "Scour vulnerability of River Bridges Piers". *J. Geotech. Geoenviron. Eng*., 129 (10), 890-900.

Hong, J. H., Guo, W. D., Chiem Y-M., Chen C.H. (2016). "A new practical method to simulate flood-induced bridge pier scour-A case study of Mingchu bridge piers on the Cho-Shui River." *Water*, 8. 238.

Link, O., Castillo, C., Pizarro, A., Rojas, A., Ettmer, B., Escauriaza, C., and Manfreda, S. (2017). "A model of bridge pier scour during flood waves." *J. Hydraul. Res*., 55(3), 310-323.

Liu, X., and García, M. H. (2008). "Three-dimensional numerical model with free water surface and mesh deformation for local sediment scour." *J. WaterW. Port. Coast*, 134(4), 203-217.

Mathieu, A., Chauchat, J., Bonamy, C., and Nagel, T. (2019). "Two-Phase Flow Simulation of Tunnel and Lee-Wake Erosion of Scour below a Submarine Pipeline." *Water*, 11(8), 1727.

Nagel, T., Chauchat J., Cheng Z., Liu X. F., Hsu T. J., Bonamy C., and Bertrand. (2017). "Two-phase flow simulation of scour around a cylindrical pile." *Agu Fall Meeting. AGU Fall Meeting Abstracts*, 65-72.

Van Rijn, L. C. (1984). "Sediment Transport, Part I: Bed Load Transport.". *J. Hydraul. Eng*., 110(10):1431-1456.

Richardson, E.V., Harrison L.J., Richardson J.R., Davis S.R. (1993). "*Evaluating scour at bridges*". Publication No. FHWA-IP-90-017, FHWA.

Roulund, A., Sumer, B., Fredsøe, J., Michelsen J. (2005). "Numerical and experimental investigation of flow and scour around a circular pile." *J. Fluid. Mech*., 534, 351-401.

Su, C. C., and Lu, J. Y. (2013). "Measurements and prediction of typhoon-induced short-term general scours in intermittent rivers". *Nat. Hazard.*, 66(2), 671-687.

Sumer, B.M. and Fredsøe, J. (2002). *The Mechanics of Scour in the Marine Environment*. World Scientific.